Complex Sliding Surface Based on Genetic Algorithm and Integral Compensation for Improving Solar Inverter Performance

En-Chih Chang[1], Yow-Chyi Liu[2], and Kuo-Yuan Liao[1]
[1]Department of Electrical Engineering, I-Shou University, Kaohsiung City, Taiwan, R.O.C.
[2]Department of Electrical Engineering, Kao Yuan University, Kaohsiung City, Taiwan, R.O.C.
Email: enchihchang@isu.edu.tw, liuyc@cc.kyu.edu.tw, isu10201017M@cloud.isu.edu.tw

***Abstract*—This paper proposes the performance improvement of the solar inverter using Complex Sliding Surface (CSS) based on Genetic Algorithm (GA) and Integral Compensation (IC). The CSS can restore incomplete system dynamics of Traditional Sliding Surface (TSS). However, the chattering and steady-state errors still exist in CSS. For solar inverter applications, the chattering causes high voltage harmonics and steady-state errors yield inaccurate tracking control. To improve the performance of solar inverter, the GA is well adopted to tune CSS's control gains so that the chattering can be removed. Simultaneously, steady-state errors can be eliminated by the addition of the IC. With the proposed approach, the system yields a solar inverter with high-quality AC output voltage under nonlinear and transient loading conditions. Experiments are given to verify the efficacy of the proposed approach. Because the proposed approach is simpler to implement than prior methods and offers more precise tracking control, this paper will be of interest to designers of related renewable energy systems.**

***Index Terms*—solar inverter, Complex Sliding Surface (CSS), Genetic Algorithm (GA), Integral Compensation (IC), voltage harmonics**

I. Introduction

The solar inverters gain more and more attention, and have been extensively used in energy conversion systems [1]. The solar inverters require obtaining high-quality AC output voltage of low Total Harmonic Distortion (THD) and fast dynamic response, and these can be achieved by employing feedback control. It is well-known that PI controllers have been used for many years. But, PI controllers can not ensure fast and stable output voltage response [2], [3]. Many control methods have been considered in literature such as deadbeat control, repetitive control, H-infinity control, and so on. However, these methods are difficult to have both good dynamic response and low THD of output waveform [4]-[6]. Proposed in 1950's, Sliding Mode Control (SMC) has been recognized as a powerful device capable of achieving good robustness, even invariant under certain condition, with respect to system parameter variations and external load interferences [7], [8]. The control of the inverters is popularly designed via SMC. Jezernik *et al*. presents a single sliding surface function to perform all control objects, however the chattering exists [9]. Chiang *et al*. develops a multi-loop control to improve the controller presented in [9]. But, the steady-state response is unsatisfactory [10]. Chan *et al*. proposes a discrete variable structure controlled servo system. The steady-state response is satisfactory, but there is poor dynamic response [11]. Jung *et al*. presents a closed-loop scheme with large parameter variations for PWM inverter applications. Though the fast dynamic response is obtained, the inverter output voltage is distorted under rectifier loads [12]. In addition, Jung *et al*. also proposes a discrete feedforward sliding mode controlled inverter system. The fast dynamic and good steady-state response are achieved. However, the chattering around the sliding surface exists [13]. A discrete integral variable structure control is introduced by Phakamach *et al*. This controller eliminates steady-state errors, but the dynamic response is unsatisfactory [14]. As above-cited, the SMC with TSS is frequently adopted, and thus the partial system dynamics is lost. To restore lost system dynamics, the CSS is designed for solar inverters. However, the chattering and steady-state errors still exit in CSS [15], [16]. The chattering easily causes tear and wear to system components and may lead to serious voltage harmonics in solar inverter output, and steady-state errors create inaccurate tracking control. Thus, the control gains of the CSS can be properly determined by GA for removing the chattering while zero steady-state errors can be achieved by the use of the IC [17], [18]. By combining a CSS with GA and IC, a closed-loop solar inverter will yield good performance under different loading. The proposed approach is finally demonstrated by the solar inverter, and is digitally realized using a DSP and CPLD. Experimental results for the solar inverter are performed in support of the proposed approach. The paper is organized as follows: Section II describes the dynamic model of solar inverter. A CSS based on GA and IC is derived in Section III. In Section IV, the experiments for the solar inverter are performed in support of the proposed approach. Conclusions are given in Section V.

Manuscript received February 16, 2015; revised September 22, 2015.

©2015 International Journal of Electrical Energy

doi: 10.18178/ijoee.3.4.252-256

II. Mathematical Modeling of Solar Inverter

Fig. 1 displays the block diagram of a solar inverter. Suppose v_o be the output voltage, v_{ref} be the desired sinusoidal waveform, and $e_1 = v_o - v_{ref}$ be the voltage error. Then, the error dynamical matrix can be written as:

$$\begin{bmatrix} \dot{e}_1 \\ \dot{e}_2 \end{bmatrix} = \underbrace{\begin{bmatrix} 0 & 1 \\ -\frac{1}{LC} & -\frac{1}{RC} \end{bmatrix}}_{\text{system matrix}} \begin{bmatrix} e_1 \\ e_2 \end{bmatrix} + \underbrace{\begin{bmatrix} 0 \\ \frac{1}{LC} \end{bmatrix}}_{\text{control matrix}} u + \underbrace{\begin{bmatrix} 0 \\ -\frac{1}{LC} v_{ref} - \frac{1}{RC} \dot{v}_{ref} - \ddot{v}_{ref} \end{bmatrix}}_{\text{external disturbance}} \tag{1}$$

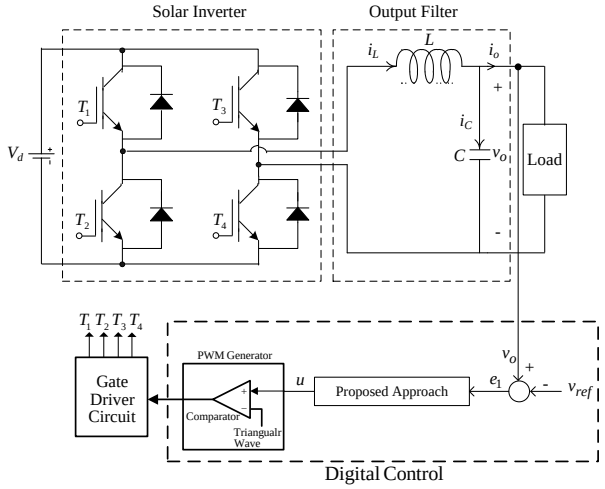

Figure 1. Block diagram of solar inverter.

Once the control signal u is designed well, the inverter's output will remain the same as what is desired v_{ref}.

III. Control Design

A. TSS

Generally, TSS is chosen as:

$$\sigma = \ker(C) \subset \Re, \text{ where } C \in \Re^{m \times n};\ rank(C) = m \tag{2}$$

The resulting closed-loop dynamics yields:

$$\begin{bmatrix} \dot{x} \\ \dot{y} \end{bmatrix} = \begin{bmatrix} \mathrm{R_e} A_z & 0 \\ 0 & \mathrm{R_e} A_z \end{bmatrix} \begin{bmatrix} x \\ y \end{bmatrix} + \begin{bmatrix} 0 \\ B \end{bmatrix} u,\ \begin{matrix} A_z = system\ matrix \\ B = control\ matrix \end{matrix} \tag{3}$$

From (2) and (3), the system dynamics is $(n-m)$ reduced-order dimension, and deteriorates system performance. To restore lost system dynamics, the CSS can be designed as follows.

B. CSS Design

We define the u and x with the pairs of complex conjugate ($v, \bar{v}$ and $z, \bar{z}$) as:

$$u = \frac{1}{2}(v + \bar{v}) \tag{4}$$

$$x = \frac{1}{2}(z + \bar{z}) \tag{5}$$

where $v, \bar{v} \in C^m$ and $z, \bar{z} \in C^n$.

Substituting (4) and (5) into (3), the real system (3) yields the sum of the two complex system:

$$\dot{z} = Az + Bv \tag{6}$$

$$\dot{\bar{z}} = A\bar{z} + Bv \tag{7}$$

A complex valued switching surface is introduced as:

$$\gamma = \Psi z = 0 \tag{8}$$

$$z = \begin{bmatrix} x_1 & \cdots & x_m & \dot{x}_1 & \cdots & \dot{x}_m \end{bmatrix}^T \tag{9}$$

where $\Psi \in C^{m \times n}$.

The sliding function matrix in the regular form (2) is partitioned compatibly as:

$$\Psi = \begin{bmatrix} \Psi_1 & \Psi_2 \end{bmatrix} = \begin{pmatrix} M_{11} + iN_{11} & & 1 & & \\ & \ddots & & \ddots & \\ & & M_{mm} + iN_{mm} & & 1 \end{pmatrix} \tag{10}$$

where $\Psi_1 \in C^{m \times (n-m)}$ and $\Psi_2 \in C^{m \times m}$.

The system matrix becomes:

$$A_z = (I - B(\Psi B)^{-1}\Psi)A = \begin{bmatrix} A_{11} - A_{12}\Psi_2^{-1}\Psi_1 & A_{12} \\ 0 & 0 \end{bmatrix} \tag{11}$$

Setting $z = x + iy$, we have:

$$\begin{aligned} \dot{\bar{z}} + \dot{z} &= A_z(x + iy) + \bar{A}_z(x - iy) \\ &= 2(\mathrm{Re}\, A_z x - \mathrm{I_m} A_z y) \end{aligned} \tag{12}$$

i.e.,

$$\dot{x} = \mathrm{Re}\, A_z x - \mathrm{I_m} A_z y \tag{13}$$

$$y = \frac{1}{2}(z + \bar{z}) \tag{14}$$

Contrariwise,

$$\begin{aligned} \dot{\bar{z}} - \dot{z} &= A_z(x + iy) + \bar{A}_z(x - iy) \\ &= 2(\mathrm{I_m} A_z x + \mathrm{Re}\, A_z y) \end{aligned} \tag{15}$$

i.e.,

$$\dot{y} = \mathrm{I_m} A_z x + \mathrm{Re}\, A_z y \tag{16}$$

Hence, the $\Re^{2n}$ dimensional system exists:

$$\begin{bmatrix} \dot{x} \\ \dot{y} \end{bmatrix} = \begin{bmatrix} \mathrm{R_e} A_z & -\mathrm{I_m} A_z \\ \mathrm{I_m} A_z & \mathrm{R_e} A_z \end{bmatrix} \begin{bmatrix} x \\ y \end{bmatrix} \tag{17}$$

It is easy to verify the conventional situation where Ψ is a real linear map, that is, $\Psi = \sigma$, then the (17) has:

$$\begin{aligned} \begin{bmatrix} \dot{x} \\ \dot{y} \end{bmatrix} &= \begin{bmatrix} \mathrm{R_e} A_z & 0 \\ 0 & \mathrm{R_e} A_z \end{bmatrix} \begin{bmatrix} x \\ y \end{bmatrix} \\ &= \begin{bmatrix} (I - B(CB^{-1}C)A & 0 \\ 0 & (I - B(CB^{-1}C)A \end{bmatrix} \begin{bmatrix} x \\ y \end{bmatrix} \end{aligned} \tag{18}$$

The control signal is assumed have the form:

$$v = \underbrace{-(\Psi B)^{-1}\Psi Az}_{u_{ez}} \underbrace{-(\Psi B)^{-1}\Psi Az\left[F\text{sign}(\mathrm{R}_e(\gamma)+iG\text{sign}(\mathrm{I}_m(\gamma))\right]}_{u_{swz}} \quad (19)$$

where u_{ez} is the equivalent control and u_{swz} represents a discontinuous switching control component.

Defining $v = u + iw$, (4) and (19) lead to:

$$u = -\mathrm{R}_e(\Psi B)^{-1}\Psi Ax + \mathrm{I}_m(\Psi B)^{-1}\Psi Ay - \mathrm{R}_e(\Psi B)^{-1}F\,\text{sign}(\mathrm{R}_e\gamma) + \mathrm{I}_m(\Psi B)^{-1}G\,\text{sign}(\mathrm{I}_m\gamma) \quad (20)$$

and

$$w = -\mathrm{I}_m(\Psi B)^{-1}\Psi Ax + \mathrm{R}_e(\Psi B)^{-1}\Psi Ay - \mathrm{I}_m(\Psi B)^{-1}F\,\text{sign}(\mathrm{R}_e\gamma) - \mathrm{R}_e(\Psi B)^{-1}G\,\text{sign}(\mathrm{I}_m\gamma) \quad (21)$$

Assuming $\Psi = M + iN$, the (20) and (21) is rearranged as:

$$\begin{bmatrix} u \\ w \end{bmatrix} = -\begin{bmatrix} \mathrm{R}_e(\Psi B)^{-1}\Psi A & \mathrm{I}_m(\Psi B)^{-1}\Psi A \\ \mathrm{I}_m(\Psi B)^{-1}\Psi A & \mathrm{R}_e(\Psi B)^{-1}\Psi A \end{bmatrix}\begin{bmatrix} x \\ y \end{bmatrix} + \begin{bmatrix} \mathrm{R}_e(\Psi B)^{-1}F & \mathrm{I}_m(\Psi B)^{-1}G \\ \mathrm{I}_m(\Psi B)^{-1}F & \mathrm{R}_e(\Psi B)^{-1}G \end{bmatrix} \cdot \text{sign}\left(\begin{bmatrix} M & -N \\ N & M \end{bmatrix}\begin{bmatrix} x \\ y \end{bmatrix}\right) \quad (22)$$

Applying $y = 1/2(z - \bar{z})$, the differential equation is expressed as:

$$\dot{y} = Ay + Bw \quad (23)$$

The resulting system is shown in (24) into $\Re^{2n}$ dimension, and thus restores all the dynamics lost in the TSS.

$$\begin{bmatrix} \dot{x} \\ \dot{y} \end{bmatrix} = \begin{bmatrix} \mathrm{R}_e A_z & -\mathrm{I}_m A_z \\ \mathrm{I}_m A_z & \mathrm{R}_e A_z \end{bmatrix}\begin{bmatrix} x \\ y \end{bmatrix} + \begin{bmatrix} B & 0 \\ 0 & B \end{bmatrix}\begin{bmatrix} u_{ez} \\ w_{swz} \end{bmatrix} \quad (24)$$

where the u_{ez} denotes equivalent control, and the w_{swz} is sliding control. Thus, the presented control law is $u_{ez} + iw_{swz}$.

The (24) implies sign function, and thus has a chattering problem. To remove chattering, the control gains of the complex sliding surface can be tuned by GA as follows.

C. GA Tuning

1) Initial population

An initial population is constructed as:

$$x(n) = x_{\min}(n) + rand \times (x_{\max}(n) - x_{\min}(n)), \quad n = 1, 2, ..., j \quad (25)$$

where *rand* is bounded by 0 and 1, and $x_{\min}(n)$ and $x_{\max}(n)$ are minimum and maximum values, respectively.

2) Fitness function

The objective function, J is designed as:

$$J = \int_0^\infty (W_1|x_{e1}| + W_2 u^2)dt \quad (26)$$

where W_1 and W_2 are both weight values. Then, the fitness function, F is selected in connection with J that indicates as $F = 1/J$.

3) Selection

Assume the generation size be g, the adaptive degree of individual k be $F(k)$, the proportion of individual k yields:

$$P(k) = F(k)\Big/\sum_{k=1}^{g} F(k), \quad k = 1, 2, ..., g \quad (27)$$

4) Crossover

Randomly select a crossover site, K_{cr} within $0 \le K_{cr} < M$, then by keeping the genes of the parent creatures between position 1 and K_{cr} unaltered and interchanging the genes of the parent creatures between position $K_{cr}+1$ and M two new creatures can be obtained as:

$$x^{cr,\,z,\,p} = \alpha x^{s,\,z,\,p}(n) + (1-\alpha)x^{s,\,z,\,q}(n) \quad (28)$$

$$x^{cr,\,z,\,q} = (1-\alpha)x^{s,\,z,\,p}(n) + \alpha x^{s,\,z,\,q}(n) \quad (29)$$

where n is bounded by $K_{cr}+1$ and M, and $0 \le \alpha \le 1$.

5) Mutation

The $(z+1)$th population can be created by using the mutation operation as follows.

$$x^{z+1,\,p}(n) = x^{cr,\,z,\,p}(n) + \beta\zeta_n \quad (30)$$

where β is bounded by -1 and 1, and ζ_n is the mutation amplitude of the nth gene.

D. Integral Compensation

Notice that the (1) with external disturbances still causes steady-state errors, and thus an IC $u_{ic} = \int e_1 dt$ is introduced to overcome steady-state errors. Finally, the proposed control law is $u = u_{ic} + u_{ez} + iw_{swz}$.

TABLE I. SYSTEM PARAMETERS

DC-bus Voltage V_d	240V
Output Voltage v_c	110V_{rms}
Output Frequency f	60Hz
Filter Inductor L	0.5mH
Filter Capacitor C	40μF
Switching Frequency f_s	15kHz
Rated Load R	12Ω

IV. EXPERIMENTAL RESULTS

This section is devoted to the verifying of the proper operation of the proposed approach through experimental results. The proposed system parameters are given in Table I. For no load to full load, the results with the proposed approach and TSS are shown in Fig. 2 and Fig. 3, respectively. The output voltage with the proposed approach only dips lightly, but the large voltage sag occurs in the TSS. For rectifier loading (200μF capacitor in parallel with a 20Ω resistor) shown in Fig. 4, the

output voltage with the proposed approach is almost sinusoidal waveform (%THD=1.62%), but that with the TSS shown in Fig. 5 has a high %THD of 9.42%. Table II lists output-voltage %THD under step load change and rectifier load.

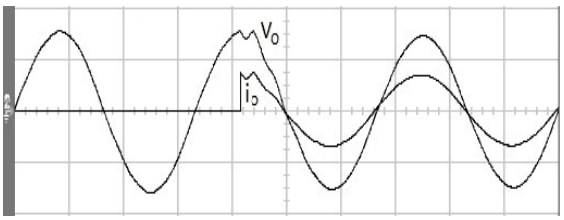

Figure 2. Solar inverter output waveforms from no load to full load with the proposed approach (100V/div; 20A/div; 5ms/div).

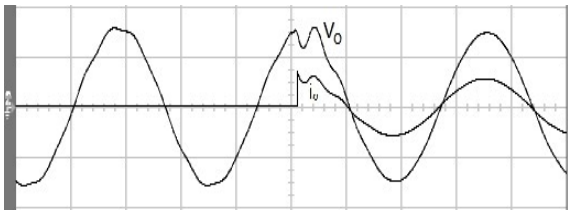

Figure 3. Solar inverter output waveforms from no load to full load with the TSS (100V/div; 20A/div; 5ms/div).

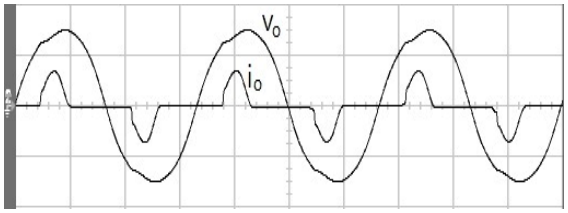

Figure 4. Solar inverter output waveforms under rectifier load with the proposed approach (100V/div; 40A/div; 5ms/div).

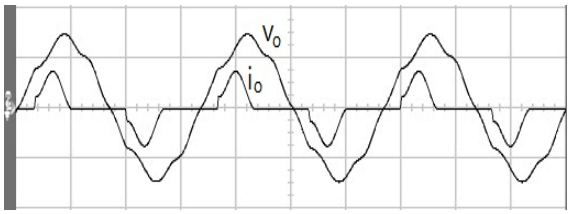

Figure 5. Solar inverter output waveforms under rectifier load with the TSS (100V/div; 40A/div; 5ms/div).

TABLE II. EXPERIMENTAL OUTPUT-VOLTAGE %THD UNDER STEP LOAD CHANGE AND RECTIFIER LOAD

	Proposed Approach		Classic TSS	
Loading	Step Load Change	Rectifier Load	Step Load Change	Rectifier Load
%THD	3.63%	1.62%	25.79%	9.42%

V. CONCLUSIONS

The proposed inverter restores lost system dynamics, removes chattering, and overcomes steady-state errors. Even under severe nonlinear loads, the high-quality solar inverter output with low total harmonic distortion and fast dynamic response can be obtained. There is no denying that the proposed approach has robustness to parametric uncertainties, and external disturbances. Experimental results show that the presented system surpasses the results achieved under the traditional system.

ACKNOWLEDGMENT

This work was supported by the Ministry of Science and Technology of Taiwan, R.O.C., under contract number MOST103-2221-E-214-027. Also, Yow-Chyi Liu is the equal contribution author.

REFERENCES

[1] N. Mohan, T. M. Undeland, and W. P. Robbins, *Power Electronics: Converters, Applications, and Design*, New York, USA: Wiley, 2003.
[2] J. Selvaraj and N. A. Rahim, "Multilevel inverter for grid-connected PV system employing digital PI controller," *IEEE Trans. on Industrial Electronics*, vol. 56, no. 1, pp. 149-158, 2009.
[3] J. Dannehl, F. W. Fuchs, and P. B. Thøgersen, "PI state space current control of grid-connected PWM converters with LCL filters," *IEEE Trans. on Power Electronics*, vol. 25, no. 9, pp. 2320-2330, 2010.
[4] Y. I. Mohamed, M. Rahman, and R. Seethapathy, "Robust line-voltage sensorless control and synchronization of LCL-filtered distributed generation inverters for high power quality grid connection," *IEEE Trans. on Power Electronics*, vol. 27, no. 1, pp. 87-98, 2012.
[5] D. Chen, J. M. Zhang, and Z. M. Qian, "An improved repetitive control scheme for grid-connected inverter with frequency-adaptive capability," *IEEE Trans. on Industrial Electronics*, vol. 60, no. 2, pp. 814-823, 2013.
[6] M. Howlader, N. Urasaki, A. Yona, T. Senjyu, and A. Y. Saber, "Design and implement a digital H-infinity robust controller for a MW-class PMSG-based grid-interactive wind energy conversion system," *Energies*, vol. 6, pp. 2084-2109, 2013.
[7] S. C. Tan, Y. M. Lai, and C. K. Tse, *Sliding Mode Control of Switching Power Converters: Techniques and Implementation*, Boca Raton, FL, USA: CRC Press, 2012.
[8] Y. Shtessel, C. Edwards, L. Fridman, and A. Levant, *Sliding Mode Control and Observation*, New York: Springer, 2014.
[9] K. Jezernik and D. Zadravec, "Sliding mode controller for a single phase inverter," in *Proc. IEEE APEC'90*, 1990, pp. 185-190.
[10] S. J. Chiang, T. S. Tai, and T. S. Lee, "Variable structure control of UPS inverters," *Proc. IEE-Elect. Power Applicat.*, vol. 145, no. 6, pp. 559-567, 1998.
[11] C. Y. Chan, "Servo-System with discrete-variable structure control," *Syst. Contr. Lett.*, vol. 17, no. 4, pp. 321-325, 1991.
[12] S. L. Jung and Y. Y. Tzou, "Sliding mode control of a closed-loop regulated PWM inverter under large variations," in *Proc. IEEE Int. Conf. Power Electronics Specialists Conference*, 1993, pp. 616-622.
[13] S. L. Jung and Y. Y. Tzou, "Discrete feedforward sliding mode control of a PWM inverter for sinusoidal output waveform synthesis," in *Proc. IEEE Int. Conf. Power Electronics Specialists Conference*, 1994, pp. 552-559.
[14] P. Phakamach and C. Akkaraphong, "Microcontroller-Based discrete feedforward integral variable structure control for an Uninterruptible Power System (UPS)," in *Proc. IEEE Int. Conf. Power Electronics Specialists Conference*, 2003, vol. 2, pp. 1422-1427.
[15] B. M. Shepit and J. K. Pieper, "Sliding-Mode control design for a complex valued sliding manifold," *IEEE Trans. Autom. Contr.*, vol. 48, no. 1, pp. 122-127, 2003.
[16] X. H. Yu and J. X. Xu, *Variable Structure Systems: Towards the 21st Century*, New York: Springer-Verlag, 2002.
[17] H. M. Hasanien and S. M. Muyeen, "Design optimization of controller parameters used in variable speed wind energy conversion system by genetic algorithms," *IEEE Trans. Sustainable Energy*, vol. 3, no. 2, pp. 200-208, 2012.
[18] S. Abdel-Khalik, G. S. Mostafa, M. I. Masoud, and B. W. Wiliams, "Optimum flux distribution with harmonic injection for a multiphase induction machine using genetic algorithms," *IEEE Trans. Energy Conversion*, vol. 26, no. 2, pp. 501-512, 2011.

©2015 International Journal of Electrical Energy

En-Chih Chang was born in Kaohsiung, Taiwan, in 1975. He received the B.S. degree from Feng-Chia University, Taichung, Taiwan, R.O.C., in 1999, the M.S. degree from National Taiwan Ocean University, Keelung, Taiwan, R.O.C., in 2001, and the Ph.D. degree from National Cheng Kung University, Tainan, Taiwan, R.O.C., in 2008, all in electrical engineering. He joined the Department of Electrical Engineering, I-Shou University in 2009 as an Assistant Professor. His research interests include sliding mode control, intelligent control, grey theory, and their applications in power electronics systems.

Yow-Chyi Liu was born in Kaohsiung, Taiwan. He received his M.S., and Ph.D. degrees in electrical engineering from National Chen-Kung University, Tainan, Taiwan, R.O.C., in 1994, and 2005, respectively. He is currently an Assistant Professor in the Department of Electrical Engineering, Kao Yuan University, Kaohsiung City, Taiwan. His research interests include power electronics, electric vehicles, battery, and rapid transit system.

Kuo-Yuan Liao received B.S. degree in electronic engineering from I-Shou University, Dashu District, Kaohsiung City, Taiwan, R.O.C., in 2013, where he is currently working toward the M.S. degree in the Department of Electrical Engineering. His research interests include the field of power electronics.

©2015 International Journal of Electrical Energy